The fine scale convection in the boundary layer mode is called "fingers." Fingers in aqueous NH_4Cl appear before channels form, but when the channels and their plumes develop the fingers disappear. Hence, if the same sequence occurs in Pb-Sn alloys, then our channels would appear to simulate reality. Of course, channels are three-dimensional, but Neilson and Incropera[4] indicate that channels can be simulated by both two and three dimensional calculations. Finally, if our so-called pockets are channels, then their lifetimes are too short. Channels in both metallic alloys and aqueous NH_4Cl solutions persist over much longer distances.[2,6] Felicelli *et al.*[3] showed that channels within the mushy zone persist when flow lateral to the wall of the channel is inhibited. This suggests that a mechanism involving a large reduction of permeability at the wall of the channel might be responsible for stabilizing the internal channels.

ACKNOWLEDGEMENTS

The authors are grateful to NASA-MSAD for the support of this work. Computations were done at the San Diego Supercomputer Center with a grant provided by CRAY Research Inc. The code was developed by Dr. S. Felicelli, now with Centro Atomico Bariloche in Argentina. Mr. N. Kulkarni, graduate student, and Dr. J. Crempien of the University of Concepcion, Chile, ably assisted the authors.

REFERENCES

1. A. F. Giamei and B. H. Kear, "On the Nature of Freckles in Nickel Base Superalloys," *Metall. Trans.*, 1 (1970), 2185-2192.
2. J. R. Sarazin and A. Hellawell, "Channel Formation in Pb-Sn, Pb-Sb and Pb-Sn-Sb Alloy Ingots and Comparisons with the System NH_4Cl-H_2O," *Metall. Trans. A*, 19A (1988), 1861-1871.
3. S. D. Felicelli, J. C. Heinrich and D. R. Poirier, "Simulation of Freckles during Vertical Solidification of Binary Alloys," *Metall. Trans. B*, 22B (1991), 847-859.
4. P. G. Neilson and F. P. Incropera, "Unidirectional Solidification of a Binary Model Alloy and the Effects of Induced Fluid Motion," Report No. DOE/ER/13759-5, Jan. 19, 1992.
5. S. M. Copley, A. F. Giamei, S. M. Johnson and M. F. Hornbecker, "The Origin of Freckles in Unidirectionally Solidified Castings," *Metall. Trans.*, 1 (1970), 2193-2204.
6. A. K. Sample and A. Hellawell, "The Effect of Mold Precession on Channels and Macrosegregation in Ammonium Chloride-Water Analog Castings," *Metall. Trans. B*, 13B (1984), 495-501.
7. V. R. Voller and C. Prakash, "A Fixed Grid Numerical Modelling Methodology for Convection/Diffusion Mushy Region Phase Change Problems," *Inter. J. Heat and Mass Transfer*, 30 (1987), 1709-1719.
8. W. D. Bennon and F. P. Incropera, "The Evolution of Macrosegregation in Statically Cast Binary Ingots" *Metall. Trans. B*, 18B (1987), 611-616.
9. C. Beckermann and R. Viskanta, "Double-Diffusive Convection during Dendritic Solidification of a Binary Mixture," *Physico-Chemical Hydrodynamics*, 10 (1988), 195-213.
10. M. G. Worster, "Instabilities of the Liquid and Mushy Regions during Solidification of Alloys," *J. Fluid Mech.*, (1991), in press.
11. S. D. Felicelli, J. C. Heinrich and D. R. Poirier, "Numerical Model for Dendritic Solidification of Binary Alloys," *Numerical Heat Transfer*, (1992), accepted for publication.
12. J. T. Mason, J. D. Verhoeven and R. Trivedi, "Primary Dendrite Spacing, I. Experimental Studies," *J. Crys. Growth*, 59 (1989), 516-524.

MODELING OF THE MUSHY ZONE EVOLUTION DURING DIRECTIONAL DENDRITIC GROWTH INTO AN UNDERCOOLED MELT

A. Ludwig, D. Ma, P.R. Sahm

Foundry Institute
of the
Rhine-Westphalian Institute of Technology
FRG - 5100 Aachen

ABSTRACT

Based on an analytical approach for describing the solute diffusion in the course of columnar dendritic growth, a numerical simulation of the mushy zone evolution during the autonomous directional single crystal solidification have been attempted. Assuming a cylindrical geometry, the longitudinal and the radial growth of the dendrites has been modeled simultaneously. Cooling curves, fraction solid, and the temperature distribution within the casting are calculated for various conditions. The influence of different temperature gradients on the mushy zone evolution during autonomous directional solidification has been assessed.

INTRODUCTION

In order to predict the microstructure formation of equiaxed solidification M. Rappaz and P. Thévoz 1987 have proposed an appropriate model (1). In contrast to previous work (2, 3, 4) they consider the solute diffusion at the scale of a grain, which they assume to be spherical. Based on the overall thermal and solutal balance their model predicts cooling curves including recalescence, the time evolution of radial concentration profile, and the increase in fraction solid within the dendritic grain volume. In a further paper they simplify the model resulting in a relation between the internal fraction f_i and the supersaturation Ω (5). This simplified version could be easily implemented in FEM temperature solvers (6).

At the Foundry-Institute in Aachen single crystal turbine blades made of superalloys have been produced by the so-called autonomous directional solidification (ADS) (7). In this technique a single crystal solidifies from an undercooled melt, resulting in a columnar dendritic structure with dendrites more than 100 mm in length (8). Thus, the assumption of spherical grains can not be used in this case. In the present paper a suitable model for describing the structural evolution and the thermal history during the ADS process is proposed.

Modeling of Casting, Welding and
Advanced Solidification Processes VI
Edited by T.S. Piwonka, V. Voller and L. Katgerman
The Minerals, Metals & Materials Society ©1993

PROCESS MODELING

For the autonomous directional solidification process, shell molds which are made of SiO_2-free ceramics covered inside with a nucleation inhibiting amorphous layer are used. After casting the melt into the shell mold, the heater device is switched off. The temperature of the melt decreases, and, due to the amorphous front layer, the nucleation is delayed, leading to a substantial undercooling. The isolated water cooled chillplate at the bottom of the shell mold ensures a longitudinal temperature gradient within the melt and the nucleation to occur at the coldest position within the foot of the specimen. The isolation between the metal and the chillplate is realized with a ceramic plug. According to the thickness of this plug the termperature gradient can vary between nearly zero and more than 1 K/mm. Both limiting cases can lead to a single crystal solidification (9). Figure 1 shows the geometry of a cylindrical sample solidified as a single crystal by ADS with the corresponding cooling curves measured at various positions. The cooling rate within the melt is about $\dot{T} = 0.25$ K/s and the temperature gradient is $G = 0.82$ K/mm. The solidification starts at the bottom of the specimen with an undercooling of about $\Delta T_{Nu} = 30$ K.

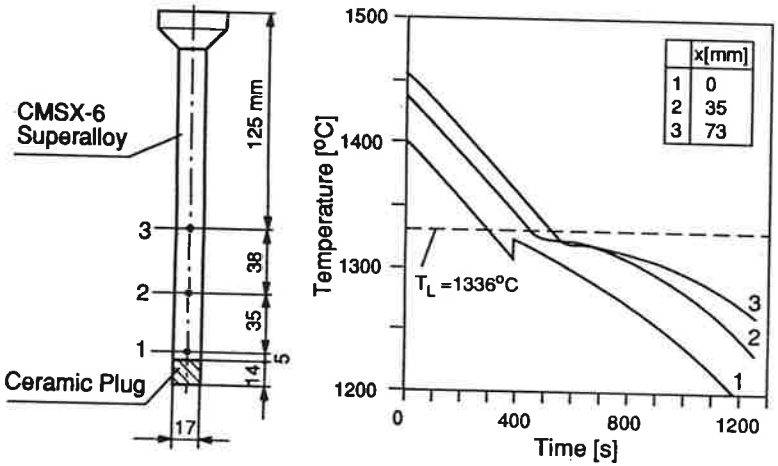

Figure 1: Specimen geometry of a single crystal produced by ADS and cooling curves measured at different positions.

The single crystal produced by ADS consists of several large columnar dendrites (9). Within the present model, it is assumed that the dendritic growth is parallel to the specimen axis and that the same growth conditions can be applied for each dendrite. The longitudinal and the lateral growth is considered separately. Because of the geometry of the problem cylindrical coordinates are used.

According to W. Kurz and D.J. Fisher 1989 (10) the following relation between the growth rate v and the undercooling at the dendrite tip ΔT^* has been used:

$$v = \frac{D}{\pi^2 \Gamma k \Delta T_0} \Delta T^{*2} \qquad (1)$$

where D is the diffusion and Γ the Gibbs-Thomson coefficient, k is the distribution coefficient and ΔT_0 the solidification interval.

The corresponding tip radius R is given by (10)

$$R = 2\pi \left(\frac{D\Gamma}{\Delta T_0 k v} \right)^{\frac{1}{2}} . \qquad (2)$$

The longitudinal growth of the dendrite tip is followed by the lateral growth of the dendrite arms. In the present model the radial growth is treated as a 2D-equiaxed growth, and thus a modified 2-dimensional Rappaz-Thévoz model has been worked out. Because most of the rejected solute is pushed radially, it is assumed that the mass transport in longitudinal direction can be neglected. Thus the solute distributions within a transversal section may be said to be independent of the neighboring sections.

Considering a cylindrical volume element with a radius R_t and a thickness of unity, as shown in Fig. 2, the radial fraction of the dendritic evolution f_g and the solid fraction f_s may be related to the corresponding radii R_g and R_s by:

$$f_g = \left(\frac{R_g}{R_t} \right)^2 \qquad \text{and} \qquad f_s = \left(\frac{R_s}{R_t} \right)^2 . \qquad (3)$$

Based on similar assumptions as made by M. Rappaz and P. Thévoz (complete mixing of solute within the interdendritic liquid, uniform temperature of the grain, etc.) the solutal balance within the cylindrical volume element results in the same expressions for the internal fraction f_i and for the solute layer thickness δ.

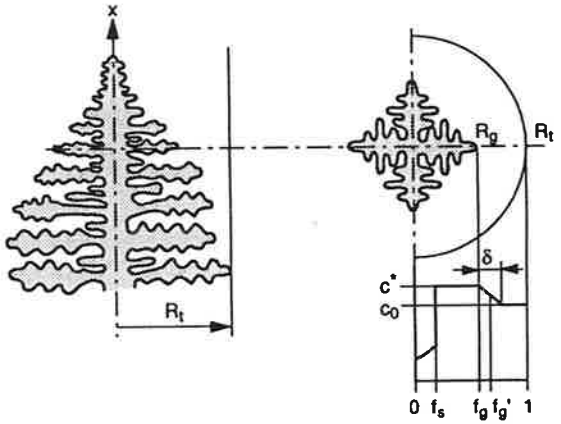

Figure 2: Schematic of the longitudinal and the transverse section of a dendrite with the corresponding solute distribution.

The following differences to the Rappaz and Thévoz model have been seen to exist. Based on the expression for solutal conservation:

$$(c^* - c_0)\,\pi\left(R_g'^2 - R_g^2\right) = \int_{R_g}^{R_g+\delta} \frac{c^* - c_0}{\delta}\left(R_g + \delta - r\right) 2\pi r \mathrm{d}r \qquad (4)$$

f_g' is related to f_g by:

$$f_g' = f_g \cdot g(z) = f_g\left(1 + Z + \frac{1}{3}Z^2\right), \qquad (5)$$

with

$$Z = \frac{\delta}{R_g}. \qquad (6)$$

f_g' is defined in Fig. 2 (R'_g is the corresponding radius). This relationship between f'_g and f_g is sligthly different to that obtained in the spherical growth model (5).

Another difference appears in the energy equation. In the present paper the conduction of heat between the various cylindrical volume elements has been included. Thus the energy equation is given by:

$$2\pi R_t Q + \pi R_t^2 \lambda \frac{\Delta^2 T}{\Delta x^2} = \pi R_t^2 \left(\rho c_p \frac{\Delta T}{\Delta t} + L \frac{\Delta f_s}{\Delta t}\right) \qquad (7)$$

in which Q is the external heat flow in lateral direction, λ the thermal conductivity, ρc_p the volumetric specific heat, L the volumetric latent heat and ΔT the change in temperature within the time step Δt. For relating the change in the supersaturation $\Delta\Omega$ to ΔT the following expression is used:

$$\Delta T = m\Delta c^* \cong \Delta\Omega\left(k\Delta T_0\right) \qquad (8)$$

Based on the above equations the evolution of T, f_g and f_s can be calculated as a function of the solidification time until the radial solute layer reaches the total lateral radius R_t. To describe dendritic impingement the solute concentration at R_t has to increase as soon as the boundary layer approaches R_t. An appropriate description has been implemented into the model.

The advance of the dendrite in longitudinal direction is calculated by using the simple relation:

$$x^n = x^o + v \cdot \Delta t \qquad (9)$$

where x^o and x^n is the old and the new tip position, respectively. The velocity has been calculated using equation (1) by considering that the tip undercooling ΔT^* is estimated by a linear interpolation between the temperatures of the neighboring transversal sections.

It is assumed that the solidification starts at the bottom of the specimen (first volume element) at an undercooling of $\Delta T_{Nu} = 15$ K with a nucleus, $R_{Nu} = 5 \cdot 10^{-6}$ µm in size. The nucleation conditions for the further cylindrical volume elements are assumed to be:

i) ΔT_{Nu} due to the temperature of the considered volume element which is reached by the longitudinal growth.

ii) R_{Nu} due to the radius of the corresponding dendrite tip.

As in the other models the presented algorithm originates from describing the microstructure evolution of binary alloys. To apply the algorithm in the case of superalloys the multi-component system has been reduced to a quasi-binary alloy (11). On this score the diffusion coefficient D is estimated by applying the constitutional undercooling criterion (12):

$$D = \frac{\Delta T_0}{(G/v)_c} \qquad (10)$$

where $(G/v)_c$ is the critical G over v value for the appearence of constitutional undercooling. G is the temperature gradient at the liquid/mushy interface. The distribution coefficent k is approximated as:

$$k = \frac{v_c}{v_t} \qquad (11)$$

in which v_c and v_t are the critical velocities for the morphological transition planar-cellular and cellular-dendritic (13).

The values of $(G/v)_c$, v_c and v_t for the superalloy CMSX-6 have been previously estimated by D. Ma 1990 (14). The resulting D and k together with other relevant physical properties of the superalloy CMSX-6 are listed in Table 1.

Table 1: Physical properties used in the calculation for the superalloy CMSX-6

liquidus temperature	$T_L = 1336$°C
diffusion coefficient	$D = 2.9 \times 10^{-9}$ m²/s
distribution coefficient	$k = 0.31$
solidification interval	$\Delta T_0 = 100$ K
heat of fusion	$L = 1.5 \times 10^9$ J/m³
Gibbs-Thomson coefficient	$\Gamma = 10^{-7}$ Km
heat capacity	$\rho c_p = 9.17 \times 10^6$ J/(m³ K)
heat conductivity	$\lambda = 30$ W/Km

RESULTS AND DISCUSSION

Figure 3 shows the calculated cooling curves and the solid fraction vs. time curves at various positions within a cylindrial specimen similar to that in Fig. 1. A cooling rate of $\dot{T}$ = 0.25 K/s and a temperature gradient of about G = 1.2 K/mm have been applied. The undercooling at the onset of solidification has been assumed to be ΔT_{Nu} = 15 K. Due to this undercooling the cooling curve, calculated at the bottom of specimen, has a remarkable recalescence. At higher positions the solidification starts with smaller undercooling, and thus the recalescence is less pronounced. This result is in good agreement with the experimental measurements (Fig. 1).

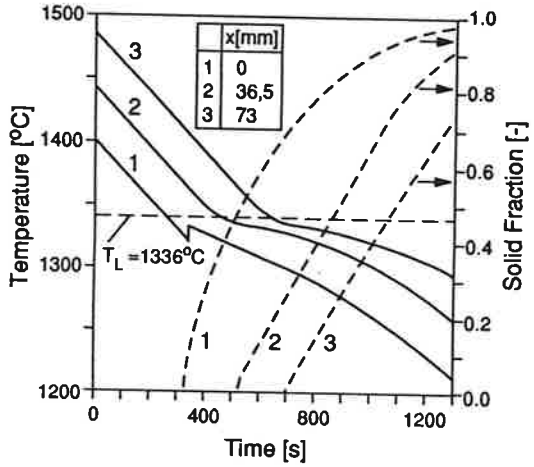

Figure 3: Calculated cooling and solid fraction curves corresponding to the thermocouple locations 1, 2 and 3 in Fig. 1.

Figure 4 shows the calculated temperature distribution and the corresponding solid fraction curves within the cylindrical sample for two different initial temperature gradients. With a large gradient of G = 1.2 K/mm the initial undercooling of about ΔT_{Nu} = 15 K is restricted to a small area at the bottom of the specimen (Fig. 4a). A recalescence can only be determined within this region (compare curve 1 in Fig. 3). Unless this initial transient the solidification rate is governed only by the heat flow - the growth condition emerge to directional solidification. As the release of latent heat reduces the temperature gradient in the mushy region, the expression $v = \dot{T}/G$ gives only an upper limit for the solidification rate. In Fig. 4a the growth rate v is about 0.19 mm/s whereas $\dot{T}/G$ is 0.21 mm/s. The solid fraction increases monotonously due to the advance of the liquid/mushy interface (Fig. 4b).

Applying a small gradient of about G = 0.01 K/mm (Fig. 4b) a quasi homogeneous undercooling within the entire specimen can be achieved before the onset of solidification. This results in uniform growth conditions along the specimen (constant growth rate, equal recalescence and uniform solid fraction evolution). The solidification rate is determined by the growth into the undercooled melt. According to equation (1) v is about 0.8 mm/s. After the longitudinal growth the entire specimen

has become a homogeneous mushy zone in which the termperature as well as solid fraction are uniform.

(a)

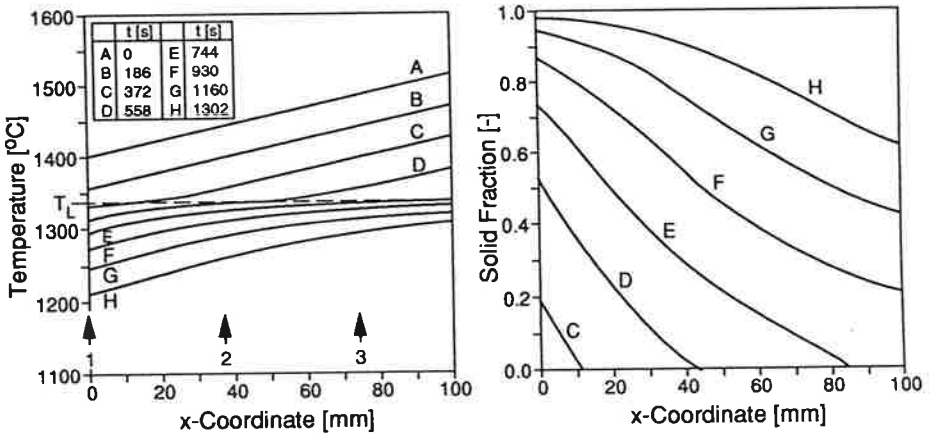

(b)

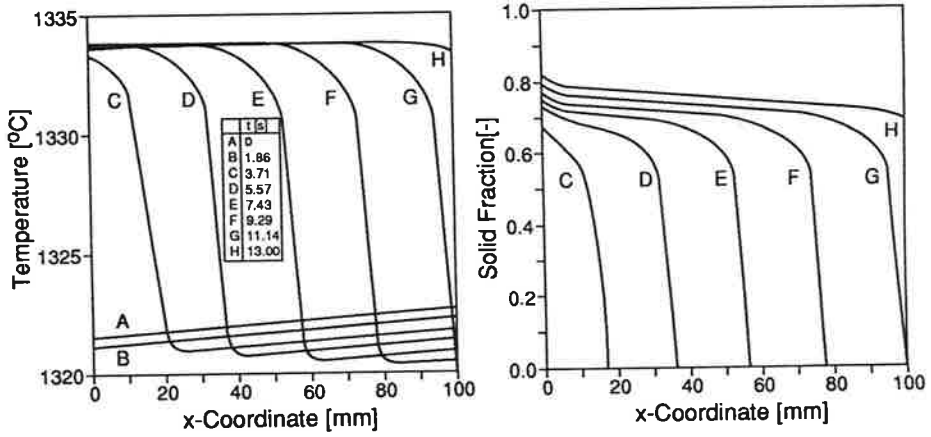

Figure 4: Calculated distribution of temperature and solid fraction along the specimen at different times for two different initial temperature gradients of G = 1.2 K/mm (a) and G = 0.01 K/mm (b). The numbered arrows in (a) correspond to the cooling curves in Fig. 3.

CONCLUSION

Based on the solid diffusion model by M. Rappaz and P. Thévoz 1987 an approach has been made to study the lateral growth of the dendrite arms in the mushy zone during autonomous directional solidification. A modified cylindrical model was proposed in which the longitudinal growth of the dendrite axis and the heat accumulation in longitudinal direction was considered. The calculated cooling curves at various locations show different depth of recalescence which is also observed in the measurements.

ACKNOWLEDGEMENT

The authors would like to acknowledge to Dr. J. Stanescu for numerous discussions concerning ADS experiments and for measuring the cooling curves in Fig. 1.

REFERENCES

1. M. Rappaz and Ph. Thévoz, Acta Metall. 35 (1987) 1487
2. I. Dustin and W. Kurz, Z. Metallk. 77 (1986) 265
3. J. D. Hunt, Mater. Sci. Engng. 65 (1984) 75
4. S. C. Flood and J. D. Hunt, Proc. of Int. Conf. on Modelling of Casting and Welding Processes III, Santa Barbara, California (1986) 607
5. M. Rappaz and Ph. Thévoz, Acta Metall. 35 (1987) 2929
6. Ph. Thévoz, J. L. Desbiolles, M. Rappaz, Met. Trans. A 20 (1989) 311
7. J. Stanescu and P.R. Sahm, Ingenieur-Werkstoffe 2 (1990) 64
8. J. Stanescu, P.R. Sahm, J. Schädlich-Stubenrauch, A. Ludwig, Proc. of Int. Conf. on Investment Casting VII, Las Vegas, Nevada (1992)
9. J. Stanescu, Dr.-Ing. Dissertation, RWTH Aachen (1992)
10. W. Kurz and D. J. Fisher, "Fundamentals of solidification", Trans. Tech. Publ. Aedermannsdorf, Switzerland (1989)
11. D. Ma and P.R. Sahm, Gießereiforschung 42 (1990) 122
12. W.A. Tiller, K. A. Jackson, R. W. Rutter, B. Chalmers, Acta Metall. 1 (1953) 428
13. W. Kurz and D. J. Fisher, Acta Metall. 29 (1981) 11
14. D. Ma. "Solidification Behaviour of Ni-Based Superalloys", VDI-Verlag GmbH, Düsseldorf, Germany (1990)

A complete model for microsegregation during columnar dendrite growth

András Roósz, Assistant Professor
University of Miskolc, Physical Metallurgy Department
Egyetemváros, H-3515, Miskolc, Hungary
Hans Eckart Exner, Professor
Technical University of Darmstadt, Faculty of Materials Science
Petersenstr. 30, D-6100 Darmstadt, Germany

ABSTRACT

A model for the prediction of microsegregation during steady state solidification is developed which includes all known kinetic effects on solute distribution (back diffusion, secondary dendrite arm coarsening, primary tip and eutectic undercooling and thermodynamical correction of the interface temperature). The numerical procedure is outlined. As an example, the magnitude of the various effects on the homogenisation is demonstrated for an Al-1wt%Si alloy for a wide range of cooling rates. The results of the numerical predictions are compared with experimental results for two aluminium alloys (Al-1wt%Si and Al-4.9wt%Cu) showing the good performance of the model.

INTRODUCTION

The first successful approach to predict microsegregation in binary alloys due to Scheil (1) was followed by many attempts to improve the validity with respect to boundary conditions and kinetic effects. In the most advanced models (Brody and Flemings (2), Clyne and Kurz (3), Kirkwood and Evans (4), Feest and Doherty (5), Roósz et al (6), Basharan (7), Roósz and Exner (8), Battle and Pehlke (9), Sarreal and Abbaschian (10) one or more of the following effects are still neglected :

- back diffusion in the solid phase
- secondary dendrite arm coarsening
- primary dendrite tip undercooling (solutal and kinetical undercooling, curvature effect, thermodynamical correction of interface temperature)
- eutectic undercooling.

In this presentation we will show a model in which we consider all these contributions for steady state dendritic growth.

THE MODEL

The symbols used in the following are defined in the list al the end of this paper. The calculation considers dendritic solidification at a constant temperature gradient G at the primary dendrite tip which moves with a constant velocity v into the melt. Dendrite tip

Modeling of Casting, Welding and
Advanced Solidification Processes VI
Edited by T.S. Piwonka, V. Voller and L. Katgerman
The Minerals, Metals & Materials Society ©1993